Journal of Magnetic Resonance 210 (2011) 210–217

Contents lists available at ScienceDirect

Journal of Magnetic Resonance

journal homepage: www.elsevier.com/locate/jmr

DEER in biological multispin-systems: A case study on the fatty acid binding to human serum albumin

Matthias J.N. Junk, Hans W. Spiess, Dariush Hinderberger *

Max Planck Institute for Polymer Research, Ackermannweg 10, 55128 Mainz, Germany

ARTICLE INFO

Article history:
Received 23 September 2010
Revised 14 December 2010
Available online 10 March 2011

Keywords:
Multispin systems
Double electron–electron resonance (DEER)
Dipolar couplings
Spin labels
Protein structure determination

ABSTRACT

In this study, self-assembled systems of human serum albumin (HSA) and spin-labeled fatty acids are characterized by double electron–electron resonance (DEER). HSA, being the most important transport protein of the human blood, is capable to host up to seven paramagnetic fatty acid derivatives. DEER measurements of these self-assembled multispin clusters are strongly affected by correlations of more than two spins, the evaluation of the latter constituting the central topic of this paper. While the DEER modulation depth can be used to obtain qualitative information of the number of coupled spins, the quantitative analysis is hampered by the occurrence of cluster mixtures with different numbers of coupled spins and contributions from unbound spin-labeled material. Applying flip angle dependent DEER measurements, unwanted multispin correlations were found to lead not only to a broadening of the distance peaks but also to cause small distances to be overestimated and large distances to be suppressed. It is thus favorable to use spin-diluted systems with an average of two paramagnetic molecules per spin cluster when a quantitative analysis of the distance distribution is sought.

1. Introduction

While there is an ever increasing demand to characterize the structure of disordered macro- and supramolecular (biological) systems in the nanometer range, pulse electron paramagnetic resonance (EPR) spectroscopy is among the few methods that are capable of providing quantitative information on this length scale [1]. The most commonly used method is referred to as double electron–electron resonance (DEER) or pulsed electron–electron double resonance (PELDOR) spectroscopy and utilizes the inherent distance dependence of the dipolar couplings between unpaired electron spins to access distances in the range of 1.5–8 nm [2–5]. In recent years, the four-pulse DEER experiment has almost become a standard technique to characterize both synthetic [6,7] and biological systems [8] with the focus on (membrane) proteins and nucleic acids [9–13].

In most studies, the application of DEER was enabled by site-specific mutagenesis of the biomacromolecule and subsequent attachment of two spin labels [14,15]. By variation of these sites and repeated distance measurements, information about the three dimensional conformation of the system can be inferred by triangulation. For these doubly labeled mutants, the approximation of well separated spin pairs is valid and standard procedures to convert the experimental data into distance distributions can be applied [16,17]. However, when a single cluster contains more than two spins, for instance trimers of singly labeled proteins [18,19], additional modulations of the time-domain signal due to couplings to more than one spin might be observed.

In the early days of EPR distance measurements, the inversion efficiency and thus the probability to invert more than one spin with the pump pulse was low. But even at that time it was noted that the depth of the dipolar modulation was influenced by the number of coupled spins in a cluster [3]. This concept of spin counting was rigorously tested on model radicals by Bode et al. [20]. With increasing microwave power and the increasing use of DEER not only for well-defined spin pair systems, it became necessary to explicitly identify and remove the effect of multispin contributions on distance distributions. This was achieved by Jeschke et al. [21], who utilized the different dependency of *N*-spin interactions on the inversion efficiency of the pump pulse to separate the spectral contribution due to spin pair correlations from three-spin correlations [21].

Recently, we used a fully self-assembled system of human serum albumin (HSA) and spin-labeled fatty acids (see Fig. 1) to determine the protein's functional structure in solution [22]. Albumin is the most abundant protein in human blood plasma and serves as a transporting agent for various endogenous compounds and drug molecules [23,24]. Its capability to bind and transport multiple fatty acids is of particular importance [25,26]. Crystallographic

* Corresponding author. Fax: +49 6131 379 100.
E-mail address: dariush.hinderberger@mpip-mainz.mpg.de (D. Hinderberger).

1090-7807/$ - see front matter © 2011 Elsevier Inc. All rights reserved.
doi:10.1016/j.jmr.2011.03.003

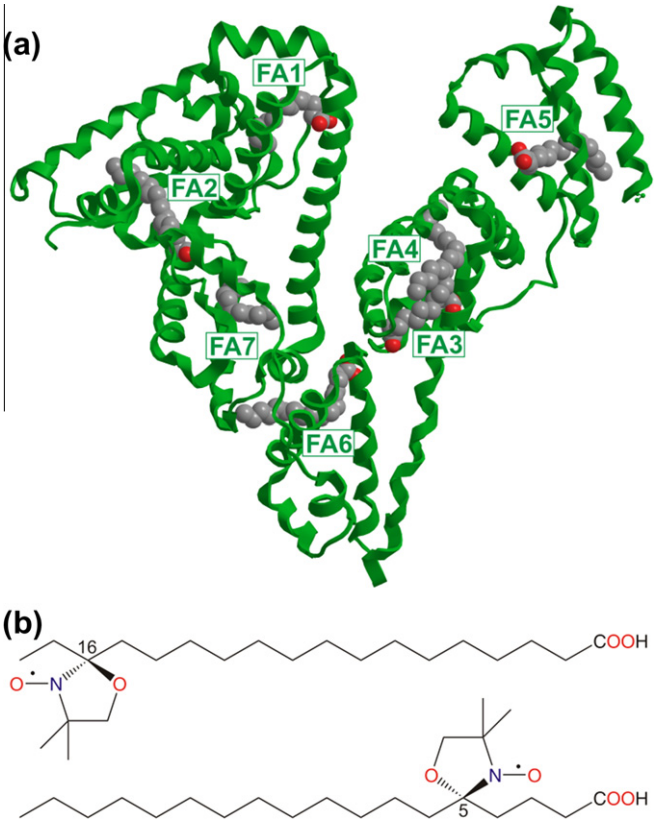

Fig. 1. (a) Crystal structure (PDB 1e7i) of HSA co-crystallized with seven stearic acid molecules [29]. The oxygen atoms of the FA carboxylic acid head groups are displayed in red. (b) Chemical structure of the EPR active molecules, 5-doxylstearic acid (DSA) and 16-DSA. (For interpretation of the references to color in this figure legend, the reader is referred to the web version of this article.)

analyses of HSA–fatty acid complexes revealed up to seven distinct binding sites for long chain fatty acids, most of which comprised of ionic anchoring units and long, hydrophobic pockets [27–30].

5-Doxylstearic acid (5-DSA) and 16-DSA were applied to sample the ionic anchor points in the protein's interior (5-DSA) as well as the entry points into the fatty acid channels (16-DSA), respectively. We found that the anchor points are asymmetrically distributed in the rigid interior of the protein and largely in agreement with the distribution found from the crystal structure. In clear contrast to the crystal structure, we found the binding sites' entry points to be distributed homogeneously and symmetrically on the protein's surface. This was attributed to a large conformational flexibility in solution which facilitates the uptake and release of fatty acids [22]. These results were obtained with spin-diluted HSA–fatty acid systems. Different amounts of diamagnetic fatty acids were admixed to the protein and the EPR-active DSA molecules to enable a variation of the fatty acid loading of the protein while limiting the average number of electron spins in the cluster to two. Thus, artifacts in the distance distribution due to multispin correlations were avoided.

In this paper, we study in detail how the DEER data are affected when the protein is solely loaded with spin-labeled fatty acids, i.e. when multiple paramagnetic centers are clustered in the protein. In the first part, the spin counting formalism is applied to quantify the number of coupled spins, followed by a discussion of the limitations of this method for self-assembled systems. In the second part, we apply flip angle dependent DEER measurements to identify artifacts in the distance distributions due to multispin contributions, which hamper the correct interpretation of the distance data and may lead to erroneous conclusions. The exact analysis is especially important for self-assembled systems with a large variety of possible conformations, which result in complicated distance distributions.

2. Results and discussion

2.1. Spin counting

The intramolecular parts of the DEER time-domain data are shown in Fig. 2a when the protein is loaded with 1–8 paramagnetic 16-DSA molecules (the raw DEER data is displayed in the Supplementary data, Section 2). The DEER curve for a 16-DSA/HSA ratio of 2:1 exhibits a pronounced cosine modulation with a characteristic frequency of ~1 MHz. This is indicative of the fatty acids molecules being located in protein binding channels, which are separated by a dominating, well-defined distance. This dominant modulation, though slightly less distinct, persists when the 16-DSA/HSA ratio is increased, i.e. when the protein is loaded with additional spin-labeled fatty acids. At the same time, the modulation depth Δ, illustrated graphically in Fig. 2a and defined by

$$\Delta = 1 - \lim_{t\to\infty} V(t)/V(0) \tag{1}$$

increases. The conversion of the time-domain data of systems with more than two spins into quantitative distance distributions and the associated problems are discussed in detail in the second part of the Section 2. In the following, we will evaluate to what extent the modulation depth can be used to provide information about the system.

The modulation depth provides a means to quantify the fatty acid molecules per protein by the determination of the number of dipolar coupled spins N [3]. N can be inferred by the relation [20],

$$N = \frac{\ln(1-\Delta)}{1-\lambda} + 1, \tag{2}$$

where λ is the inversion efficiency of the pump pulse. As mentioned above, the modulation depth increases as more spin-labeled fatty acid equivalents are added to the protein (Fig. 2a). It reaches a constant value for HSA–fatty acid ratios $\geqslant$1:5. As expected, the increase of the average number of spins per protein molecule is reflected in the increase of the modulation depth.

The modulation depth Δ can be readily determined from the background corrected DEER time trace. The inversion efficiency λ of the pump pulse can, in principle, be calculated provided that the amplitude and duration of the pump pulse and the EPR lineshape are known [18,31]. This method is, however, prone to several sources of errors. Hence, it is common to experimentally access the inversion efficiency through the modulation depth of a biradical (N = 2, thus $\Delta = \lambda$) [16].

In this study, an inversion efficiency of λ = 0.52 was determined using a rigid phenylene–ethynylene based biradical with a spin–spin distance of 2.8 nm [32]. All experimental conditions were kept constant for the biradical and the HSA–fatty acid complexes to allow for comparability of the inversion efficiency [16]. When the modulation depth of the DSA/HSA DEER data was, however, referenced with respect to the biradical, the calculated average number of coupled spins varied from 1.49 (for a 1:2 mixture of HSA and 16-DSA) to 2.81 (for a 1:6 mixture of HSA and 16-DSA) (Table 1).

This result suggests that the protein is not able to complex more than three fatty acid molecules on average even if up to eight DSA molecules are available per HSA molecule. This observation clearly disagrees with CW EPR data on these samples and with well-established results in the HSA literature. Using CW EPR spectroscopy, we found that even at a HSA–fatty acid ratio of 1:6, the fatty acid uptake is almost quantitative with more than 99.7% of all fatty

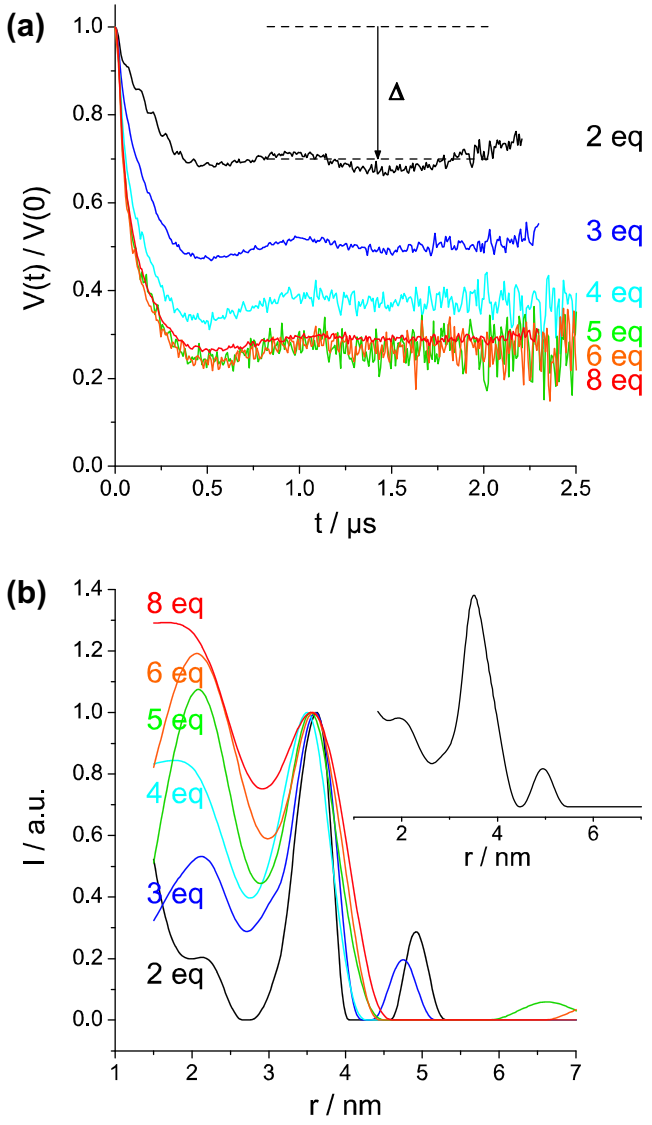

Fig. 2. (a) Background corrected DEER time-domain data of HSA complexed with 2–8 equivalents of 16-DSA with a graphical illustration of the definition of the modulation depth Δ. The raw time-domain data are shown in the Supplementary data, Section 2. (b) Corresponding distance distributions by Tikhonov regularization with a regularization parameter of 100 normalized to the height of the peak at 3.6 nm. The 'real' 16-DSA distance distribution in a fully fatty acid loaded HSA molecule is shown in the inset. This distribution was obtained from a spin-diluted system with six diamagnetic fatty acids and two paramagnetic 16-DSA molecules per protein molecule [22].

Table 1
Modulation depths Δ and average numbers of spins N in HSA–fatty acid complexes.

	Biradical	HSA: 16-DSA					
		1:2	1:3	1:4	1:5	1:6	1:8
Δ	0.516	0.300	0.497	0.626	0.728	0.730	0.708
N (Ref: biradical)	2.0	1.49	1.94	2.36	2.80	2.81	2.70
N (Ref: 1:2)	–	2.0	2.93	3.76	4.65	4.67	4.45

acids being complexed by the protein [22]. This finding is supported by crystallographic studies, which identified up to seven different binding sites for long chain fatty acids [29]. In an earlier titration study, which assumed only five binding sites, very strong stearic acid association constants of $>3.5 \times 10^7$ were determined for each binding site [25]. In essence, the number of coupled fatty acid is largely underestimated for all HSA–fatty acid complexes by DEER spin counting with a rigid biradical as reference. Apparently, a rigid biradical in *o*-terphenyl is not a good choice to calibrate the inversion efficiency for our self-assembled biological samples in an aqueous environment.

We note that the modulation depth of doubly labeled protein mutants is often considerably smaller than the expected modulation depth for rigid biradicals. The common reasoning of incomplete spin-labeling being responsible for this apparent deviation does not always seem adequate. For instance, studying the folding of the light harvesting membrane protein LHCII by DEER, the depth of the dipolar modulation was as low as 0.2, although fluorescence experiments suggested that more than 80% of all protein mutants carried two spin labels [9,33].

The apparent discrepancy between the inversion efficiency for the rigid biradical and our self-assembled biological samples could be due to various reasons. First of all, the biradical possesses a slightly narrower EPR spectrum than the doxyl-labeled fatty acids in the protein (Supplementary data, Section 1). The increased spectral density at the maximum of this slightly narrower biradical spectrum leads to the excitation of a higher fraction of spins by the pump pulse and to a slight increase of the inversion efficiency. Further, the rigid geometry of the biradical causes the inversion efficiency to be orientation dependent. In a recent study, the modulation depth of similar rigid biradicals was revealed to differ significantly even at X-band depending on where the observer pulse was placed in the nitroxide spectrum [11]. These angular correlations are absent in case of our biological samples as checked by field-swept DEER measurements (Supplementary data, Section 3). Most importantly, though, our self-assembled systems of a biological host and paramagnetic guests typically consist of a mixture of clusters with different amounts of paramagnetic centers since each HSA molecule is able to accommodate up to seven spin-labeled fatty acid molecules. For instance, a 2:1 mixture of 16-DSA and HSA, in which all spin-labeled fatty acids are bound to the protein, consists of a distribution of protein clusters with 0, 1, 2, 3 (and a higher number of) incorporated fatty acids. Although the overwhelming number of clusters will have two DSA molecules bound to HSA, all these clusters contribute to the overall DEER signal (with the exception of the pure protein without incorporated fatty acids). However, their contribution is weighted with a scaling factor which is related to the transverse relaxation time T_2 of the spins in the cluster [20]. A cluster with a small number of paramagnetic centers possesses a larger relaxation time than a cluster with a larger number of paramagnetic centers and thus contributes to a greater extent to the DEER data (Supplementary data, Section 1).

Hence, a protein complex with one incorporated fatty acid contributes to the DEER signal to a higher degree than, e.g., a protein complexed with three 16-DSA molecules. For the 2:1 mixture of 16-DSA and HSA, this weighting of the different contributions causes the modulation depth to indicate a number of coupled spins $N < 2$ although two fatty acids are bound to HSA on average.

We note that, in principle, the modulation depth can also be partly suppressed for dipolar pairs with short distances and dipole–dipole couplings in the range of or larger than the excitation bandwidth of the pump pulse [16]. This source of error can be excluded for the studies in this paper. As explained in detail in Ref. [22], the labeled C-16 positions of fatty acids are distributed homogeneously on the protein surface in solution with a main distance contribution at 3.6 nm. Further, no indications for strong dipolar couplings can be found in ESE detected spectra as spectral broadenings are absent (Supplementary data, Section 1).

In conclusion, the calibration of the inversion efficiency by a rigid biradical leads to erroneous numbers of coupled spins for our self-assembled system. We note that the above-mentioned

numbers of coupled spins are reproducibly obtained for a series of different inversion efficiencies (Supplementary data, Section 5). To obtain more meaningful spin counting results, a reference is needed which resembles the properties of the self-assembled systems.

In a particularly simple approach, we approximated the inversion efficiency of the pump pulse by the modulation depth of a 2:1 mixture of 16-DSA and HSA ($\Delta = 0.3$) instead of the model biradical. Advantages of this approach include the use of the same spin probe and environment leading to comparable spectral shapes and relaxation times. As further shown by CW EPR spectroscopy, all fatty acids are complexed by the protein. Hence, the protein clusters contain two fatty acid molecules on average. Like all other self-assembled biological samples in this study, it contains a distribution of clusters with different numbers of coupled spins. For the latter reason, the 2:1 mixture of 16-DSA and HSA should not be regarded as a classical reference to calibrate the inversion efficiency.

With the 2:1 mixture of 16-DSA and HSA as reference, DEER revealed 2.93, 3.76, and 4.65 spins per protein cluster for protein mixtures with 3, 4, and 5 equivalents of fatty acids. This result correlates well with the expected average number of fatty acids per molecule and reflects both the literature data and the CW EPR observations. Yet, the DEER-derived values are slightly lower than the theoretically expected values. This deviation is still small for the three-spin cluster, but becomes ever more apparent as the number of coupled spins increases. The apparent deviation of N towards lower values is related to the fact that the self-assembled samples consist of a distribution of clusters with different numbers of coupled spins and relaxation times. As mentioned above, protein clusters with a small number of paramagnetic centers contribute to a greater extent to the overall DEER signal than clusters with many paramagnetic moieties. The distribution of clusters is still narrow in a 2:1 sample of 16-DSA and HSA but will broaden as the protein is loaded with an increasing number of fatty acids. A broad distribution augments the influence of relaxation time dependent weighting and drives the modulation depths and numbers of coupled spins to apparently lower values.

For even higher amounts of spin-labeled fatty acid molecules per HSA molecule, the obtained values deviate significantly from the expected values (4.67 vs. 6 and 4.45 vs. 8). In addition to the relaxation time dependent decrease of the modulation depth due to a larger contribution of clusters with a small number of paramagnetic moieties, the modulation depth is additionally decreased by contributions from free, uncomplexed spin probes. These free spin probes do not contribute to the intramolecular part of the DEER signal ($\Delta = 0$), and even small fractions lead to a significant decrease of the overall modulation depth. This effect is most prominent for the 8:1 mixture, which exhibits an even smaller modulation depth than the sample containing a 6:1 mixture of 16-DSA and HSA. This is in agreement with CW EPR studies showing that the fraction of unbound DSA is substantially increased for the 8:1 mixture. The decrease of the modulation depth due to free DSA was already previously observed for the corresponding spin-diluted systems [22]. The addition of diamagnetic fatty acid molecules to mixtures of HSA and DSA lead to an increasing fraction of unbound DSA and to a decrease of the modulation depth.

Further (minor) effects which might hamper the correct determination of N include slight changes of the EPR spectra depending on the protein loading with fatty acids (Supplementary data, Section 1) and slight variations of excluded volume effects, which cause the apparent dimensionality of the exponential background to decrease for proteins with high fatty acid loadings (Supplementary data, Section 4). The first effect leads to a slight underestimation of N for HSA mixtures with a high ratio of 16-DSA, while the latter effect causes N to be slightly overestimated.

In conclusion, the modulation depth serves as a means to qualitatively assess the average number of spins in self-assembled systems. A quantitative interpretation is mainly hampered by the occurrence of spin clusters with a varying number of coupled spins and contributions from unbound spin-labeled material, both of which decrease the modulation depth. In this study, large deviations are observed for $\geqslant 5$ coupled spins in a total of seven potential binding sites even if a self-assembled system is chosen as reference.

2.2. Quantification of multispin artifacts

The distance distributions in Fig. 2b are obtained by conversion of the DEER time-domain data of the self-assembled multispin systems. When two 16-DSA molecules are added to the protein, the well-defined distance peak at 3.6 nm dominates the distance distribution. Besides this distance, two less intense peaks centered at 2.2 nm and 4.9 nm are observed. A subsequent increase of the number of DSA molecules per protein causes significant changes in the distance distribution. The intensity of the peak at the highest distance (4.9 nm) decreases until it becomes undetectable for HSA–fatty acid mixtures with more than three equivalents of DSA. Likewise, the addition of higher amounts of spin-labeled fatty acids causes a steady broadening of the dominating peak at 3.6 nm. However, the biggest changes are associated with the low distance peak at 2.2 nm. The relative height (and weight) of this peak steadily increases as more spin-labeled fatty acids are added to the system. At a ratio of 5:1 (DSA:HSA) the originally very small peak at 2.2 nm matches the height of the previously dominating peak at 3.6 nm. At a ratio of 8:1, this peak represents the dominating contribution to the distance distribution.

In summary, the distance distributions in Fig. 2b suggest that the addition of a higher number of fatty acids leads to a broadening of the distance peaks and to an increased population of short distances. However, we previously showed that the distance distribution undergoes only minor changes when HSA is loaded with different amounts of fatty acid [22]. In the previous study, we limited the number of EPR-active fatty acids to two, while varying the degree of HSA loading by addition of diamagnetic fatty acid analogs. By applying these spin-diluted systems, we were able to circumvent unfavorable multispin effects. The corresponding distribution for a system fully loaded with six diamagnetic fatty acid molecules (rDSA) and two paramagnetic 16-DSA molecules is shown in the inset of Fig. 2b. Note the large deviation of this distance distribution from the distribution obtained for an 8:1 mixture of 16-DSA and HSA. The only difference in the corresponding systems is the number of EPR-active molecules per cluster while the total number of fatty acids per HSA molecule was kept constant.

Hence, it is the multispin interactions that crucially distort the DEER data. As demonstrated by this example, this may lead to severe misinterpretations of the data if the multispin effects are not accounted for appropriately. In fact, it warrants a more detailed study to shed light on the consequences of multispin interactions on DEER distance distributions.

The first (and up to date the only) detailed study on multispin interactions was done by Jeschke et al. [21]. In this paper, the authors introduced a method to identify three-spin interactions and to account for and remove their contribution from the distance distribution. The experiment is based on the dependence of N-spin contributions on the inversion efficiency, which can roughly be approximated by

$$V_{N-spin} \propto \lambda^{N-1}. \quad (3)$$

The reader is referred to Ref. [21] for a detailed description of the theoretical background. Each N-spin contribution is affected to a different degree by a variation of the inversion efficiency, which can be controlled by the flip angle of the pump pulse. Hence, a series of measurements at different flip angles allows for the separation of the N-spin interactions. Using model bi- and triradicals, Jeschke et al. demonstrated how to separate two- and three-spin correlations and thus to obtain artifact-free distance distributions [21].

In the following, we utilize this method to reveal the effects of multispin contributions on the DEER data of self-assembled biological systems, specifically on 3:1 mixtures of 5-DSA or 16-DSA and HSA. Since three-spin interactions constitute the by far dominant part of the multispin interactions for $\lambda \ll 1$, the influence of N-spin contributions of higher order can be neglected.

Intramolecular DEER time-domain signals for six different flip angles of the pump pulse are shown in Fig. 3a and b. The flip angles were varied by selective attenuation of the microwave power of the pump pulse channel and the resulting inversion efficiencies were quantified by an inversion recovery sequence. Note that the inversion efficiencies λ_{exp} determined by this method are proportional but not identical to the inversion efficiency of the pump pulse λ for the actual DEER experiments. λ_{exp} characterizes the inversion efficiency of selected spin packets in a narrow frequency range, while λ quantifies the average inversion efficiency for the pumped spins.

The relation of the modulation depth and the inversion efficiency is given by the relation [21]

$$\Delta(\lambda) = \sum_{i=1}^{N-1} d_i \lambda^i. \tag{4}$$

For pure two-spin contributions a linear relationship is expected. Any contribution from multispin interactions gives rise to deviations from this linear dependency due to the admixture of higher order polynomials. Indeed, a slight deviation from a straight line is observed for 3:1 mixtures of both 5-DSA and 16-DSA with HSA (Fig. 3c and d). This deviation is absent if the ratio between the spin-labeled fatty acid and the protein is decreased to 2:1 (data not shown). This clearly indicates that multispin interactions contribute to the overall DEER signal. The deviation from the linear curve is not as strong as expected for a triradical [21], since the sample contains a mixture of proteins with one, two, three, and potentially higher amounts of incorporated spin-labeled fatty acids.

Having visualized the contributions due to multispin interactions, one can now focus on the resulting artifacts in the respective distance distributions. For this purpose, pair and three-spin contributions are extracted from the raw DEER data. The following considerations apply to the case of three coupled spins. In this case, the normalized DEER time-domain signal can be written as [21]

$$V(t)/V(0) = (1-\lambda)^2 + \lambda(1-\lambda)P(t) + \lambda^2 T(t). \tag{5}$$

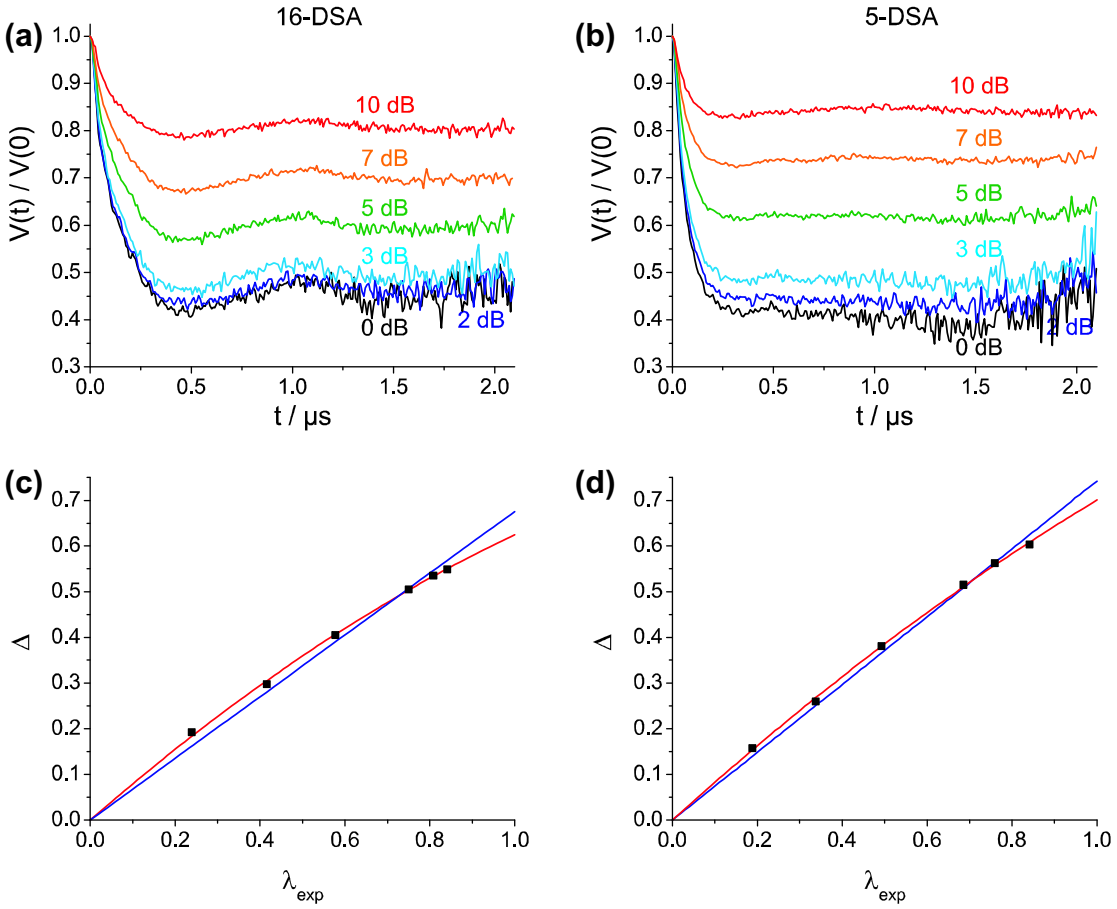

Fig. 3. (a and b) Intramolecular time-domain data of flip angle dependent DEER measurements for 16-DSA (left) and 5-DSA (right). The inversion efficiency of the pump pulse was decreased by attenuation of the microwave power output ranging from 0 dB to 10 dB. (c and d) Plots of the total modulation depth Δ as function of the inversion efficiency λ_{exp} (determined by inversion recovery). The data points were fitted with a second-order polynomial (red) accounting for two- and three-spin contributions to the DEER signal and a straight (blue) line, which neglects three-spin contributions. (For interpretation of the references to color in this figure legend, the reader is referred to the web version of this article.)

The pair contribution to the DEER signal is denoted $P(t)$, the three-spin contribution is denoted $T(t)$. The constant contribution of Eq. (5), $(1-\lambda)^2$, is related to the modulation depth Δ and can be inferred from the background fit. This contribution is eliminated for all further mathematical treatment of the data. A two-dimensional set of form factors V_{ij} with discrete times t_i and inversion efficiencies λ_j (as shown in Fig. 3) then allows the extraction of pair and three-spin contributions. The set of form factors V_i for each time t_i is fitted with a second-order polynomial with vanishing constant term [21]

$$V_i(\lambda)/V_0(\lambda) = a_i\lambda + b_i\lambda^2 = P_i\lambda + (T_i - P_i)\lambda^2. \quad (6)$$

The pair contribution is then given by $P_i = a_i$ and the three-spin contribution is given by $T_i = a_i + b_i$.

In Fig. 4, the distance distribution obtained from the pair contribution is compared to the distribution obtained from the original DEER data, which is distorted by multispin interactions.

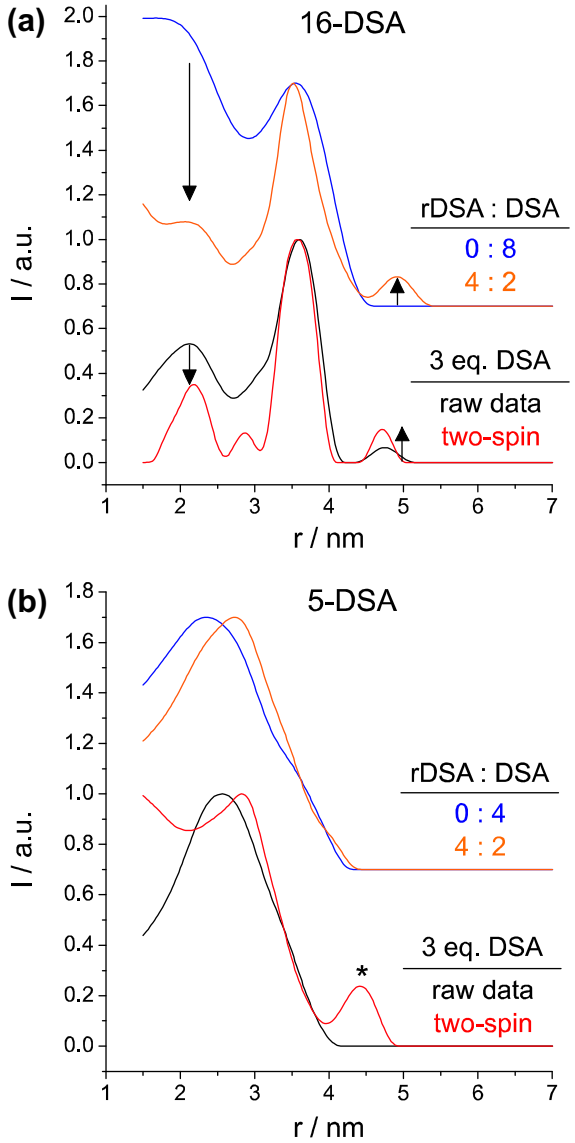

Fig. 4. Comparison of the distance distribution obtained from the raw time-domain data of a 1:3 mixture of HSA and DSA (black) and from the extracted two-spin contributions (red) for (a) 16-DSA and (b) 5-DSA. The observed differences, indicated by black arrows for 16-DSA, are compared to the deviations observed for HSA molecules fully loaded with purely paramagnetic DSA (blue) and a spin-diluted mixture of rDSA and DSA (orange). The artifact in the 5-DSA distance distribution is marked by an asterisk. (For interpretation of the references to color in this figure legend, the reader is referred to the web version of this article.)

The observed changes are most pronounced for 16-DSA, since this distribution contains well-resolved peaks but are also manifested in the distribution of 5-DSA. The multispin effects, present in the raw DEER data, lead to a slight broadening of the observed distance peaks. More severely, contributions from small distances are overestimated while large distances are suppressed. In fact, the same influence of three-spin correlations on the distance distributions is documented for the model triradicals in the study of Jeschke et al. [21].

With the data at hand, the apparent deviation between the distance distributions of fully loaded HSA samples can solely be related to multispin effects. In an 8:1 mixture of 16-DSA and HSA or in a 4:1 mixture of 5-DSA and HSA, the erroneous analysis of the raw DEER data with two- and multispin contributions leads to an overestimation of small distances and to a broadening of the peaks in full analogy to the flip angle dependent DEER results. Hence, a spin-diluted system is an indispensible prerequisite for retrieving artifact- and distortion-free distance distributions when self-assembled systems with potentially more than two paramagnetic centers are studied.

Even for protein samples with a high number of paramagnetic centers, all observed changes are well-described by three-spin contributions. It can thus be assumed that contributions from multiple spin interactions with $N > 3$ are negligible, even if as many as seven spins are coupled.

We note that also three-spin correlations, in principle, can be analyzed as they do not only contain information about the distance, but also about the relative orientation of the three interacting spins [21]. However, given the plentitude of binding sites in the protein which generate various possibilities for three-spin contributions with different distances and orientations we refrain from this analysis in the context of this study. Indeed, orientational data contain complementary information towards the distance data and could give further valuable insight into the fatty acid binding of albumin. This is more readily achieved by employing the orientational selectivity of EPR-active transition metals and constitutes the main topic of a publication which is now in preparation.

3. Conclusions

The determination of a protein structure by DEER using self-assembled systems of the unmodified protein and carefully chosen paramagnetic guest molecules offers a variety of advantages. The more technical issue that no tedious and demanding spin-labeling of the biomacromolecule is required is even surpassed by the fact that only information is obtained that is directly related to the protein's function of interest. In case of HSA, its highly relevant function to transport fatty acids can be characterized in a single experiment [22].

However, if the biological system is capable of accommodating more than two guest molecules, care must be taken that the resulting distance distributions are not prone to artifacts which originate from multispin contributions. These contributions do not only lead to a broadening of the distance peaks, but also cause small distances to be overestimated and large distances to be suppressed. It is mandatory to minimize these distortions particularly for complicated distance distributions which require exact quantitative analyses. This can be achieved by using spin-diluted systems, which contain only two EPR-active species per cluster.

Still, the modulation depth of self-assembled multispin systems contains qualitative information about the number of coupled spins. A quantitative analysis is, however, hampered by a variety of reasons, the most severe comprising the occurrence of cluster mixtures with different numbers of coupled spins and contributions from unbound spin-labeled material.

4. Experimental

4.1. Materials

Non-denaturated human serum albumin (HSA, >95%, Calbiochem), 5- and 16-doxylstearic acid (DSA, Aldrich), and 87 wt.% glycerol (Fluka) were used as received. The DSA derivatives were partly reduced to EPR-inactive hydroxylamines (rDSA) by addition of phenylhydrazine (97%, Aldrich) as described in detail in a previous publication [22].

4.2. Sample preparation

Phosphate buffered solutions (0.2 M) of pH 6.4 with and without 2 mM HSA and 6.7 mM solutions of DSA in 0.1 M KOH were mixed in the appropriate ratios to obtain HSA–fatty acid complexes in a 100 mM phosphate buffer solution of pH 7.4. Up to eight equivalents of EPR active DSA (or DSA/rDSA mixtures) were added to HSA. The concentration of DSA (or DSA/rDSA) was kept constant at 2 mM. Glycerol (20 vol.%) was added to the final solutions to prevent crystallization upon freezing. The solutions were filled into 3 mm o.d. quartz tubes and shock-frozen in $N_2(l)$ cooled *iso*-pentane (below −100 °C).

4.3. DEER measurements and analysis

Dipolar time evolution data were obtained at X-band frequencies (9.2–9.4 GHz) with a Bruker Elexsys 580 spectrometer equipped with a Bruker Flexline split-ring resonator ER4118X_MS3 using the four-pulse DEER experiment with the pulse sequence $\pi/2(\nu_{obs}) - \tau_1 - \pi(\nu_{obs}) - (\tau_1 + t) - \pi(\nu_{pump}) - (\tau - t) - \pi(\nu_{obs}) - \tau_2 -$ echo [4,5]. The dipolar evolution time t was varied, whereas τ_1 and τ_2 = 2.5 μs were kept constant. Proton modulation was averaged by addition of eight time traces of variable τ_1, starting with $\tau_{1,0}$ = 200 ns and incrementing by $\Delta\tau_1$ = 8 ns [34]. The resonator was overcoupled to $Q \approx 100$. The pump frequency ν_{pump} was set to the maximum of the EPR spectrum. The observer frequency ν_{obs} was set to ν_{pump} + 61.6 MHz, coinciding with the low field local maximum of the nitroxide spectrum. The observer pulse lengths were 32 ns for both $\pi/2$ and π pulses and the pump pulse length was 12 ns. The temperature was set to 50 K by cooling with a closed cycle cryostat (ARS AF204, customized for pulse EPR, ARS, Macungie, PA, USA). The total measurement time for each sample was around 6 h. The raw time domain DEER data were processed with the program package DeerAnalysis2008 [16]. Intermolecular contributions were removed by division by an exponential decay with a fractal dimension of d = 3.8. The deviation from d = 3.0 originates from excluded volume effects due to the size of the protein (Supplementary data, Section 4). The resulting time traces were normalized to t = 0. Distance distributions were obtained by Tikhonov regularization using regularization parameters of 100 (16-DSA) and 1000 (5-DSA).

4.4. Flip angle dependent DEER and data analysis [21]

The flip angle of the pump pulse β_{pump} was adjusted by the inversion recovery sequence $\beta_{pump} - T - (\pi/2)_{obs} - \tau - \pi_{obs} - \tau -$ echo with T = 400 ns and τ = 200 ns on the maximum of the nitroxide spectrum. A maximum inversion efficiency λ_{max} is achieved at a flip angle π_{pump}. The inversion efficiency was defined by $\lambda = 0.5(1 - I_{max}/I_{inv})$ with I_{max} being the echo amplitude without inversion by a pump pulse and I_{inv} the signed amplitude of the inverted echo. The flip angle of the pump pulse was decreased by attenuation (A) of the power output of the external microwave source with a step attenuator DC-18 GHz (Narda Microwave Corporation, New York) to obtain nominal flip angles $\beta = \pi \cdot 10^{-A/20dB}$. Attenuator settings of 0, 2, 3, 5, 7, and 10 dB were chosen for each flip angle dependent DEER experiment. The length of the pump pulse was kept at t_{pump} = 12 ns to provide for a constant excitation bandwidth. The actual experimental flip angles were calculated by $\beta = \arccos(1 - 2\lambda/\lambda_{max})$. Dipolar time evolution data for each attenuator setting were obtained with the four-pulse DEER experiment as specified in the previous paragraph. τ_2 was set to 2.2 μs for mixtures of HSA and 16-DSA and to 2.0 μs for samples containing 5-DSA. The measurement time of a single time trace was around 4 h, resulting in a total measurement time of 24 h for each sample. Intermolecular contributions were removed by division by an exponential decay with a fractal dimension of d = 3.8. Two-spin and three-spin contributions were extracted from the background-corrected time-domain data with a Matlab program kindly provided by G. Jeschke. Details of the data analysis are described in Ref. [21].

Acknowledgments

We thank Gunnar Jeschke, ETH Zurich, for providing the Matlab program for the analysis of two- and three-spin contributions and for many helpful discussions, and Christian Bauer for technical support. M.J.N.J. gratefully acknowledges financial support from the Foundation of the German chemical industry (FCI) and from the Graduate School of Excellence "Materials Science in Mainz" (MAINZ).

Appendix A. Supplementary data

ESE detected spectra for various loadings of the protein with paramagnetic fatty acids, raw DEER time-domain data field-swept DEER spectra to account for orientational effects, more detailed information about the DEER background correction, and the number of coupled spins inferred at different inversion efficiencies. Supplementary data associated with this article can be found, in the online version, at doi:10.1016/j.jmr.2011.03.003.

References

[1] G. Jeschke, Distance measurements in the nanometer range by pulse EPR, ChemPhysChem 3 (2002) 927–932.
[2] A.D. Milov, K.M. Salikhov, M.D. Shirov, Application of ENDOR in electron-spin echo for paramagnetic center space distribution in solids, Fiz. Tverd. Tela 23 (1981) 975–982.
[3] A.D. Milov, A.B. Ponomarev, Y.D. Tsvetkov, Electron-electron double resonance in electron spin echo: model biradical systems and the sensitized photolysis of decalin, Chem. Phys. Lett. 110 (1984) 67–72.
[4] M. Pannier, S. Veit, A. Godt, G. Jeschke, H.W. Spiess, Dead-time free measurement of dipole–dipole interactions between electron spins, J. Magn. Reson. 142 (2000) 331–340.
[5] G. Jeschke, M. Pannier, H.W. Spiess, Double electron–electron resonance, in: L.J. Berliner, G.R. Eaton, S.S. Eaton (Eds.), Biological Magnetic Resonance. Distance Measurements in Biological Systems by EPR, Kluwer Academic, New York, 2000, pp. 493–511.
[6] G. Jeschke, Determination of the nanostructure of polymer materials by electron paramagnetic resonance spectroscopy, Macromol. Rapid Commun. 23 (2002) 227–246.
[7] D. Hinderberger, O. Schmelz, M. Rehahn, G. Jeschke, Electrostatic site attachment of divalent counterions to rodlike ruthenium(II) coordination polymers characterized by EPR spectroscopy, Angew. Chem. Int. Ed. 43 (2004) 4616–4621.
[8] O. Schiemann, T.F. Prisner, Long-range distance determinations in biomacromolecules by EPR spectroscopy, Q. Rev. Biophys. 40 (2007) 1–53.
[9] C. Dockter, A. Volkov, C. Bauer, Y. Polyhach, Z. Joly-Lopez, G. Jeschke, H. Paulsen, Refolding of the integral membrane protein light-harvesting complex II monitored by pulse EPR, Proc. Natl. Acad. Sci. USA 106 (2009) 18485–18490.
[10] D. Hilger, H. Jung, E. Padan, C. Wegener, K.P. Vogel, H.J. Steinhoff, G. Jeschke, Assessing oligomerization of membrane proteins by four-pulse DEER: pH-dependent dimerization of NhaA Na^+/H^+ antiporter of *E-coli*, Biophys. J. 89 (2005) 1328–1338.

[11] O. Schiemann, P. Cekan, D. Margraf, T.F. Prisner, S.T. Sigurdsson, Relative orientation of rigid nitroxides by PELDOR: beyond distance measurements in nucleic acids, Angew. Chem. Int. Ed. 48 (2009) 3292–3295.
[12] O. Schiemann, N. Piton, J. Plackmeyer, B.E. Bode, T.F. Prisner, J.W. Engels, Spin labeling of oligonucleotides with the nitroxide TPA and use of PELDOR. A pulse EPR method, to measure intramolecular distances, Nat. Protocol. 2 (2007) 904–923.
[13] G. Sicoli, G. Mathis, O. Delalande, Y. Boulard, D. Gasparutto, S. Gambarelli, Double electron–electron resonance (DEER): a convenient method to probe DNA conformational changes, Angew. Chem. Int. Ed. 47 (2008) 735–737.
[14] V.W. Cornish, D.R. Benson, C.A. Altenbach, K. Hideg, W.L. Hubbell, P.G. Schultz, Site-specific incorporation of biophysical probes into proteins, Proc. Natl. Acad. Sci. USA 91 (1994) 2910–2914.
[15] W.L. Hubbell, D.S. Cafiso, C. Altenbach, Identifying conformational changes with site-directed spin labeling, Nat. Struct. Biol. 7 (2000) 735–739.
[16] G. Jeschke, V. Chechik, P. Ionita, A. Godt, H. Zimmermann, J. Banham, C.R. Timmel, D. Hilger, H. Jung, DeerAnalysis2006 – a comprehensive software package for analyzing pulsed ELDOR data, Appl. Magn. Reson. 30 (2006) 473–498.
[17] G. Jeschke, A. Koch, U. Jonas, A. Godt, Direct conversion of EPR dipolar time evolution data to distance distributions, J. Magn. Reson. 155 (2002) 72–82.
[18] J.E. Banham, C.R. Timmel, R.J.M. Abbott, S.M. Lea, G. Jeschke, The characterization of weak protein–protein interactions: evidence from DEER for the trimerization of a von Willebrand factor A domain in solution, Angew. Chem. Int. Ed. 45 (2006) 1058–1061.
[19] G. Jeschke, A. Bender, T. Schweikardt, G. Panek, H. Decker, H. Paulsen, Localization of the N-terminal domain in light-harvesting chlorophyll a/b protein by EPR measurements, J. Biol. Chem. 280 (2005) 18623–18630.
[20] B.E. Bode, D. Margraf, J. Planckmeyer, G. Dürner, T.F. Prisner, O. Schiemann, Counting the monomers in nanometer-sized oligomers by pulsed electron–electron double resonance, J. Am. Chem. Soc. 129 (2007) 6736–6745.
[21] G. Jeschke, M. Sajid, M. Schulte, A. Godt, Three-spin correlations in double electron–electron resonance, Phys. Chem. Chem. Phys. 11 (2009) 6580–6591.
[22] M.J.N. Junk, H.W. Spiess, D. Hinderberger, The distribution of fatty acids reveals the functional structure of human serum albumin, Angew. Chem. Int. Ed. 49 (2010) 8755–8759.
[23] T. Peters, All About Albumin: Biochemistry, Genetics and Medical Applications, Academic Press, San Diego, 1995.
[24] D.C. Carter, J.X. Ho, Structure of serum albumin, Adv. Protein Chem. 45 (1994) 153–203.
[25] A.A. Spector, Fatty acid binding to plasma albumin, J. Lipid Res. 16 (1975) 165–179.
[26] J.A. Hamilton, D.P. Cistola, J.D. Morrisett, J.T. Sparrow, D.M. Small, Interactions of myristic acid with bovine serum albumin: a 13C NMR study, Proc. Natl. Acad. Sci. USA 81 (1984) 3718–3722.
[27] S. Curry, H. Mandelkow, P. Brick, N. Franks, Crystal structure of human serum albumin complexed with fatty acid reveals an asymmetric distribution of binding sites, Nat. Struct. Biol. 5 (1998) 827–835.
[28] S. Curry, P. Brick, N.P. Franks, Fatty acid binding to human serum albumin: new insights from crystallographic studies, Biochim. Biophys. Acta, Mol. Cell Biol. Lipids 1441 (1999) 131–140.
[29] A.A. Bhattacharya, T. Grüne, S. Curry, Crystallographic analysis reveals common modes of binding of medium and long-chain fatty acids to human serum albumin, J. Mol. Biol. 303 (2000) 721–732.
[30] M. Fasano, S. Curry, E. Terreno, M. Galliano, G. Fanali, P. Narciso, S. Notari, P. Ascenzi, The extraordinary ligand binding properties of human serum albumin, IUBMB Life 57 (2005) 787–796.
[31] S. Ruthstein, A.M. Raitsimring, R. Bitton, V. Frydman, A. Godt, D. Goldfarb, Distribution of guest molecules in Pluronic micelles studied by double electron electron spin resonance and small angle X-ray scattering, Phys. Chem. Chem. Phys. 11 (2009) 148–160.
[32] A. Godt, C. Franzen, S. Veit, V. Enkelmann, M. Pannier, G. Jeschke, EPR probes with well-defined. Long distances between two or three unpaired electrons, J. Org. Chem. 65 (2000) 7575–7582.
[33] These experiments were conducted on the very same EPR equipment that was used in the current study, hence allowing a quantitative comparison of the data.
[34] G. Jeschke, A. Bender, H. Paulsen, H. Zimmermann, A. Godt, Sensitivity enhancement in pulse EPR distance measurements, J. Magn. Reson. 169 (2004) 1–12.